



LAWRENCE
LIVERMORE
NATIONAL
LABORATORY

Numerical Simulation of Nuclear Materials Detection, Imaging and Assay with MEGa-rays

*J. M. Hall, V. A. Semenov, F. Albert
and C. P. J. Barty*

Lawrence Livermore National Laboratory

9 June 2011

Published in *Proc. INMM, 52nd Annual Meeting (Palm
Desert, CA, 2011)*

Disclaimer

This document was prepared as an account of work sponsored by an agency of the United States Government. Neither the United States Government nor the University of California nor any of their employees, makes any warranty, express or implied, or assumes any legal liability or responsibility for the accuracy, completeness, or usefulness of any information, apparatus, product, or process disclosed, or represents that its use would not infringe privately owned rights. Reference herein to any specific commercial product, process, or service by trade name, trademark, manufacturer, or otherwise, does not necessarily constitute or imply its endorsement, recommendation, or favoring by the United States Government or the University of California. The views and opinions of authors expressed herein do not necessarily state or reflect those of the United States Government or the University of California, and shall not be used for advertising or product endorsement purposes.

Auspices Statement

This work was performed under the auspices of the U. S. Department of Energy by Lawrence Livermore National Laboratory (LLNL) under Contract DE-AC52-07NA27344.

Numerical simulation of nuclear materials detection, imaging and assay with MEGa-rays

J. M. Hall, V. A. Semenov, F. Albert and C. P. J. Barty
Lawrence Livermore National Laboratory
P.O. Box 808, M/S L-050, Livermore, CA 94550

Abstract

Once fully operational, LLNL's Nuclear Photonics Facility is expected to be capable of generating tunable, mono-energetic gamma-ray ("MEGa-ray") beams with energies of $\sim 0.5 - 2.5$ MeV and spectral intensities many orders of magnitude beyond those of current (3rd generation) synchrotron light sources. MEGa-ray beams will allow us to exploit a physical process known as nuclear resonance fluorescence (NRF), in which an energetic photon is absorbed by a nucleus, which then decays to its ground state by emitting one or more characteristic gamma rays. NRF has already been demonstrated as a potentially viable technique for detecting shielded nuclear materials in single-photon-counting experiments done with high-resolution (*e.g.* HPGe) detectors; however, the maximum count rates that these energy-differential (spectroscopic) detectors can sustain (*e.g.* < 20 kHz for moderate-sized detectors) effectively precludes their use with high-intensity photon beams such as MEGa-ray. In this paper we will present the conceptual design of an energy-integrated (*i.e.* non-spectroscopic), "Dual-Isotope Notch Observer" (DINO) NRF detection system which should be capable of detecting, imaging and assaying shielded nuclear materials (*e.g.* ^{235}U) irradiated by photon beams of arbitrary intensity by comparing the photon yields emitted at back angles from a pair of resonant (*e.g.* ^{235}U) and non-resonant (*e.g.* ^{238}U) "witness foils" located in a heavily-shielded environment downstream from the object under inspection. The ratio of the total, energy-integrated signals from scintillators recording emissions from the resonant and non-resonant foils can be used to define a robust "decision metric" that can be used in search scenarios to detect the presence of the resonant material or, given a suitable detector calibration procedure, provide accurate estimates of the aerial density ($[\text{gm}/\text{cm}^2]$) of the resonant material along the incident beam path. We have used detailed numerical simulations to investigate a number of different detection and/or imaging scenarios; however, in this paper we will focus on the potential for using MEGa-ray beams and DINO detector systems to assay conventional UO_2 fuel rods in scenarios where other assay techniques might not be as reliable or even feasible.

Introduction

Lawrence Livermore National Laboratory (LLNL) is currently engaged in the development of an intense, Compton-backscatter gamma-ray source with a very narrow bandwidth (FWHM ($\Delta E/E$) ~ 0.001) for use in the detection of Special Nuclear Materials (SNM) and isotope-specific imaging and nuclear assay applications. Once fully operational, LLNL's Nuclear Photonics Facility is expected to be capable of generating tunable, mono-energetic gamma-ray ("MEGa-ray") beams with energies of $\sim 0.5 - 2.5$ MeV and spectral intensities many orders of magnitude beyond those of current (3rd generation) synchrotron light sources [1]. In addition to their potential as basic research tools in nuclear physics, high-intensity, narrow bandwidth photon sources such as MEGa-ray are expected to have a number of applications in key LLNL research thrust areas such as homeland security (*e.g.* counter terrorism), nuclear energy and waste management, SNM safeguards (*e.g.* counter proliferation) and nuclear stockpile stewardship (*e.g.* surveillance activities).

MEGa-ray beams will allow us to exploit a physical process known as nuclear resonance fluorescence (NRF). Analogous to atomic fluorescence, NRF occurs when an energetic photon is absorbed by a nucleus, which then decays to its ground state by emitting one or more characteristic gamma rays. NRF provides unique identifying signatures for many isotopes of interest and, since the Doppler-broadened line-widths of the resonances are quite narrow (\sim few eV) compared to nuclear level spacings (\sim 100 keV), accidental interferences between different materials are unlikely. NRF cross sections are also often greater than or equal to the total atomic attenuation cross sections at the same energy, thus making it possible to penetrate $> 100 \text{ gm/cm}^2$ of surrounding material while maintaining a reasonably high sensitivity to the material of interest.

NRF has already been demonstrated as a viable technique for detecting shielded nuclear materials in single-photon-counting experiments done with high-resolution (*e.g.* HPGe) detectors [2, 3]; however, the maximum count rates that these energy-differential (spectroscopic) detectors can sustain (*e.g.* $< 20 \text{ kHz}$ for moderate-sized detectors) effectively precludes their use with MEGa-ray-like photon sources which should be capable of delivering in excess of 10^8 photons per pulse at repetition rates of $\sim 100 \text{ Hz}$ (*i.e.* $\sim 10^{10}$ photons per second). In this paper we will present the conceptual design of an energy-integrated (*i.e.* non-spectroscopic), “Dual-Isotope Notch Observer” (DINO) NRF detection system which should be capable of detecting, imaging and assaying shielded nuclear materials (*e.g.* ^{235}U) irradiated by photon beams of arbitrary intensity. We will summarize the mathematical basis for a DINO “decision metric” that will be used as a measurement diagnostic and present detailed numerical (Monte Carlo) simulations that illustrate the potential for using MEGa-ray beams and DINO detector systems to provide fast, accurate assays of conventional UO_2 fuel rods in scenarios where other assay techniques might not be as reliable or even feasible.

Conceptual design of DINO system

The conceptual design of a single-stage DINO system, which expands on NRF detection schemes originally suggested by Metzger [4] and more recently proposed by Bertozzi, *et al.* [5], is shown in Figure 1. As currently envisioned, it will consist of two separate detector elements¹. The first element will be a hemispherical scintillator (*e.g.* NaI) used to record the total, energy-integrated photon yields (beam-induced NRF + scatter) emitted into back angles (*e.g.* $\geq 90^\circ$ relative to the incident beam) from a pair of resonant and non-resonant “witness foils” located in a heavily-shielded environment downstream from the object under inspection. Since the subject of this paper is the detection, imaging and assay of nuclear materials such as ^{235}U , we will assume that we have a MEGa-ray photon source tuned to the NRF absorption in ^{235}U at $\sim 1.734 \text{ MeV}$ and somewhat arbitrarily define the resonant and non-resonant witness foils to be 1.00 cm \varnothing , 0.75 cm thick cylinders of HEU ($\sim 95 \text{ at\% } ^{235}\text{U}$, 5 at% ^{238}U) and DU ($\sim 0.20 \text{ at\% } ^{235}\text{U}$, 99.8 at% ^{238}U), respectively. The NaI scintillator will be assumed to have a nominal thickness of $\sim 40 \text{ cm}$ (*i.e.* thick enough to absorb essentially all of the $\sim 1.734 \text{ MeV}$ NRF radiation emitted by the resonant witness foil) and a high-Z (*e.g.* Ta) Compton liner $\sim 2 \text{ cm}$ thick will be used to suppress low-energy (inelastic) backscattered radiation from the witness foils. Since we will only be interested in recording the total, energy-integrated photon yields from the witness foils (*i.e.* no spectroscopic information will be required in the analy-

¹ DINO NRF detection systems (both single-stage and multi-stage designs) are protected by a continuation-in-part of U.S. Patent Application 11/528182, filed September 26, 2006, which claims priority to U.S. Provisional Application 60/720965, filed September 26, 2005. The United States Government claims rights to this technology pursuant to Contract DE-AC52-07NA27344 between the Department of Energy and Lawrence Livermore National Security, LLC.

sis), the scintillator response could, in principal, be read out in current mode, thereby allowing it to be used with incident beams of arbitrary pulse structure and intensity.

The second element in the design will be an energy-integrated beam monitor similar in composition to the first element (*e.g.* NaI). The beam monitor will be assumed to be of sufficient thickness to absorb essentially all of the residual incident beam. Its primary function will be to provide a reference level which can be used to normalize the signals obtained from the HEU and DU witness foils contained in the first element; however, in search scenarios, it can also serve as a baseline to ensure that we do not inadvertently fail to detect a threat simply because the surrounding (presumably benign) material was too thick for the incident beam to penetrate.

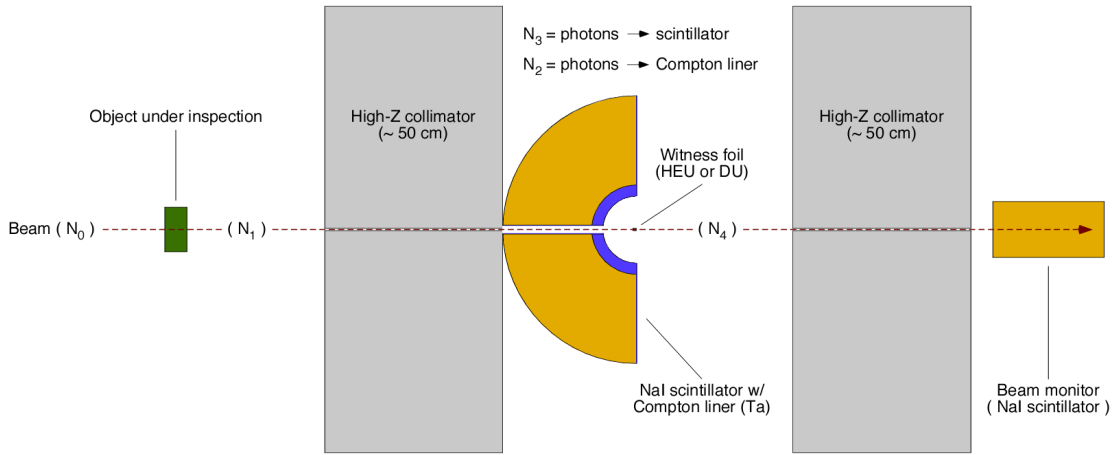


Figure 1: Conceptual design of single-stage DINO detector system. The high-Z collimators will accommodate the predicted MEGa-ray beam divergence ($\sim \pm 0.035$ mrad) while restricting the fractional solid angle for admitting background radiation from objects under inspection to less than $\sim 5\text{E-}06$. The purpose of the high-Z Compton liner on the scintillator is to suppress low-energy (inelastic) backscattered radiation from the witness foils

In transmission-mode detection schemes such as DINO, the resonant and non-resonant witness foils are used to analyze the incident photon beam *after* it passes through the object under inspection in an effort to detect a potential “notch” associated with NRF absorption by the material of interest (*e.g.* ^{235}U) in the object (*cf.* Figure 2). The NRF photon yield from the resonant foil will be inversely related to the aerial density ($[\text{gm}/\text{cm}^2]$) of the material of interest along the beam path in the object since a *high NRF yield* from the resonant foil (due to the absence of a “notch” at the resonance energy in the transmitted beam) will imply a *low resonant absorption in the object* and, thus, a *low aerial density of the material of interest*, while a *low NRF yield* from the resonant foil (due to the presence of a significant a “notch” in the transmitted beam) will imply a *high resonant absorption* in the object and, thus, a *high aerial density of the material of interest*. Non-resonant photons in the incident beam will, after proper normalization, scatter equally from both foils since Compton, Rayleigh, nuclear Thompson and Delbrück scattering do not, to first order, depend on the number of nucleons in an isotope but only on atomic number. The ratio of the total, energy-integrated signals from the resonant and non-resonant foils can therefore be used to define a “decision metric” that can be used in search scenarios to detect the presence of the resonant material or, given a suitable calibration procedure, provide fast, accurate estimates of the aerial density ($[\text{gm}/\text{cm}^2]$) of the resonant material along the incident beam path.

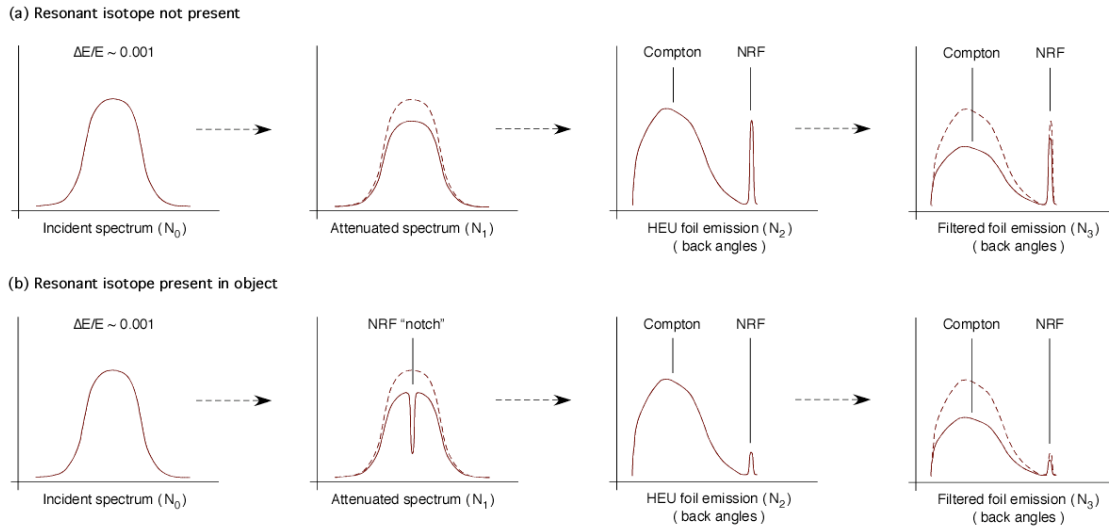


Figure 2: Conceptual evolution of photon spectra in transmission-mode DINO detector system. The top row of spectra (a) illustrates a scenario in which the resonant isotope is not present in the object under inspection, while the bottom row (b) illustrates a scenario in which the resonant isotope is present.

It should also be noted that the background radiation levels in transmission-mode detection schemes such as DINO should be relatively stable and easy to manage since the only materials in the field of view of the first detector element (the hemispherical scintillator) are the two witness foils (known quantities) and their shielding can be carefully tailored to minimize potential backgrounds from naturally-occurring radioactive materials (NORM) that might be present in the object under inspection. This feature will be particularly important when attempting to assay UO_2 fuel rods that have been removed from a reactor core after several months of operation at full power (indeed, there may be no other non-destructive assay technique that can even begin to do the job...).

Finally, we note that there are at least two different ways to expose the resonant and non-resonant witness foils in a single-stage DINO design, each having advantages and disadvantages. One way might be to use a rotating foil arrangement in which an array of resonant and non-resonant foils are alternately placed in the beam on sequential pulses. This approach has the advantage that it is relatively insensitive to minor fluctuations in beam parameters; however, it could be difficult to implement from a mechanical point of view. Another way might be to expose the resonant foil for a fixed amount of time (or a fixed amount of beam as recorded by the beam monitor) and then switch in the non-resonant foil and expose it for the same amount of time (or beam). This approach has the advantage of being relatively easy to implement from a mechanical point of view; however, it will also be somewhat more sensitive to fluctuations in beam parameters. Within the scope of this work, the exact method used to expose the witness foils will be irrelevant as long as we can assume that they are exposed for the same amount of time (or beam).

Mathematical basis for decision metric

In order to summarize the mathematical basis for the DINO “decision metric” that will be used as a measurement diagnostic, we will designate the resonant witness foil (HEU) as foil #1 and the non-resonant witness foil (DU) as foil #2 and define the following set of parameters:

$$f_s(E) = \text{photon source distribution } ([\gamma/\text{sec}/\text{MeV}]) \text{ (e.g. skewed Gaussian)}, \quad (1)$$

$$\ell_0 = \text{effective thickness of object along incident beam path}, \quad (2)$$

$$\ell_k = \text{effective thickness of HEU foil } (k=1), \text{ DU foil } (k=2), \quad (3)$$

$$n_{0,R} = \text{number density of resonant } (^{235}\text{U}) \text{ atoms in object}, \quad (4)$$

$$n_{k,R} = \text{number density of } ^{235}\text{U} \text{ atoms in HEU foil } (k=1), \text{ DU foil } (k=2), \quad (5)$$

$$n_{0,i} = \text{number density of } i^{\text{th}} \text{ atomic species in object}, \quad (6)$$

$$n_{k,U} = \text{number density of Uranium atoms in HEU foil } (k=1), \text{ DU foil } (k=2), \quad (7)$$

$$\sigma_{\text{NRF}}(E) = \text{NRF cross section for } ^{235}\text{U} \text{ (Doppler - broadened Gaussian)}, \quad (8)$$

$$\sigma_{\text{Atomic},i} = \text{total atomic cross section for } i^{\text{th}} \text{ atomic species in object} \quad (9a)$$

$$\sim \text{constant over non - zero range of } f_s(E) \quad (9b)$$

and

$$\sigma_{\text{Atomic},U} = \text{total atomic cross section for Uranium in witness foils} \quad (10a)$$

$$\sim \text{constant over non - zero range of } f_s(E). \quad (10b)$$

Given these definitions, the DINO "decision metric" (DM) can be expressed in terms of the total, energy-integrated, scintillator responses from the witness foils as

$$DM \equiv \text{Signal}_1(\text{HEU})/\text{Signal}_2(\text{DU}) [(\text{dimensionless})]$$

$$= \frac{\text{Exp}\{-\ell_0 \sum_i (n_{0,i} \sigma_{\text{Atomic},i})\} \int_E f_s(E) \text{Exp}\{-\ell_0 n_{0,R} \sigma_{\text{NRF}}(E)\} T_1(E) dE}{\text{Exp}\{-\ell_0 \sum_i (n_{0,i} \sigma_{\text{Atomic},i})\} \int_E f_s(E) \text{Exp}\{-\ell_0 n_{0,R} \sigma_{\text{NRF}}(E)\} T_2(E) dE}, \quad (11)$$

where

$$\text{Exp}\{-\ell_0 n_{0,R} \sigma_{\text{NRF}}(E)\} = \text{resonant } (^{235}\text{U} \text{ NRF}) \text{ attenuation in object}, \quad (12)$$

$$\text{Exp}\{-\ell_0 \sum_i (n_{0,i} \sigma_{\text{Atomic},i})\} = \text{total atomic attenuation in object} \quad (13)$$

and

$$T_k(E) = \text{resonant} + \text{atomic attenuation in HEU foil } (k = 1), \text{ DU foil } (k = 2) \quad (14a)$$

$$\approx 1 - \text{Exp}\{-\ell_k n_{k,R} \sigma_{\text{NRF}}(E) - \ell_k n_{k,U} \sigma_{\text{Atomic,U}}\}. \quad (14b)$$

Note that Eqn. (11) immediately reduces to

$$DM(n_{0,R} > 0) = \frac{\int_E f_S(E) \text{Exp}\{-\ell_0 n_{0,R} \sigma_{\text{NRF}}(E)\} T_1(E) dE}{\int_E f_S(E) \text{Exp}\{-\ell_0 n_{0,R} \sigma_{\text{NRF}}(E)\} T_2(E) dE}, \quad (15)$$

i.e., the total atomic attenuation in the object cancels out. This means that the decision metric should be independent of non-resonant materials in the object (*e.g.* Uranium isotopes other than ^{235}U , Oxygen atoms and various fission fragments in UO_2 fuel rods). Note also that, if the resonant isotope (^{235}U) is not present in the object (*i.e.* $n_{0,R} = 0$), then Eqn. (15) further reduces to

$$DM(n_{0,R} = 0) = \frac{\int_E f_S(E) T_1(E) dE}{\int_E f_S(E) T_2(E) dE} = DM(\text{open field}), \quad (16)$$

i.e., the resonant (NRF) attenuation in the object vanishes. This means that the decision metric for an object which does not contain the resonant isotope should be independent of both its composition and its effective thickness. These very interesting (and convenient) properties of DINO detector systems will be illustrated in the next section.

Numerical simulations

Detailed numerical simulations of the single-stage DINO detector system shown in Figure 1 were carried out using LLNL's general-purpose Monte Carlo radiation transport code, COG [6]. COG was chosen because it includes detailed, Doppler-broadened NRF absorption and emission models for actinides of interest in many SNM search and assay scenarios (*e.g.* ^{235}U , ^{238}U and ^{239}Pu); however, we should note that neither COG nor any other currently available radiation transport code includes a *complete* model for elastic photon scatter, *i.e.* a model capable of accurately simulating the *coherent combination* of Rayleigh, nuclear Thompson and Delbrück scattering, nor do they include the mechanics needed to simulate MeV-scale polarized photon sources such as MEGa-ray. With these caveats having been duly noted, we will proceed.

The photon source models used to simulate the potential use of DINO detectors in UO_2 fuel rod assay applications were based on realistic estimates developed by the MEGa-ray source design team [7]. Four different photon sources were simulated, with each being tuned to the NRF absorption in ^{235}U at ~ 1.734 MeV; however, their FWHM ($\Delta E/E$) values ranged from ~ 0.0009 to ~ 0.0049 (*cf.*

Figure 3a). Due to space restrictions, we will focus most of our discussion here on a photon source with a FWHM ($\Delta E/E$) ~ 0.0016 (*cf.* Figure 3b). This is a reasonable value thought to be achievable with MEGa-ray beams at the Nuclear Photonics Facility within the first few years of operation.

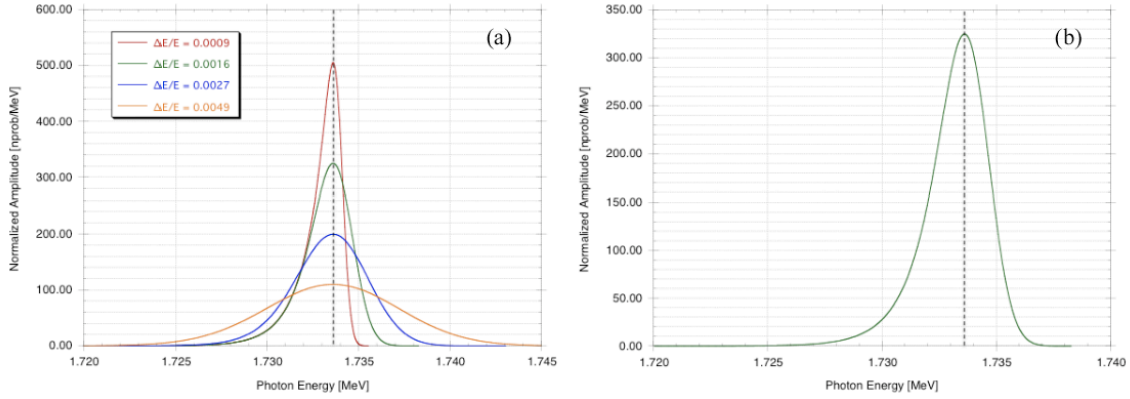


Figure 3: MEGa-ray photon sources used in Monte Carlo simulations of DINO detector systems. Frame (a) shows the range of different photon sources that have been simulated, with each being tuned to the NRF absorption in ^{235}U at ~ 1.734 MeV, while frame (b) highlights our "nominal" source, which has an effective FWHM ($\Delta E/E$) ~ 0.0016 .

In our earlier discussion of the conceptual design of a single-stage DINO system, it was noted that the purpose of the high-Z Compton liners on the DINO scintillators is to suppress low energy (inelastic) backscattered photons. Figure 4a shows an example of the photon spectrum that one might expect to observe entering the Compton liner when the HEU witness foil is irradiated by the MEGa-ray source described above and Figure 4b shows the predicted photon spectrum entering the scintillator. We note that the NRF / total ratio (which strongly influences detector sensitivity) can be driven up to $> 5\%$ using an appropriate Compton liner.

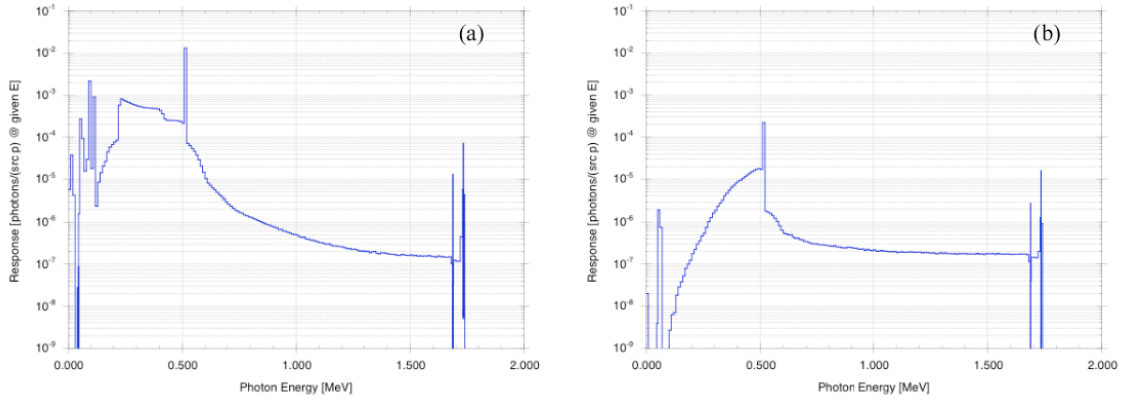


Figure 4: Predicted photon spectra entering Compton liner (a) and scintillator (b) from HEU witness foil irradiated by 1.734 MeV MEGa-ray source with effective FWHM ($\Delta E/E$) ~ 0.0016 . Note that the Rayleigh component of the elastically scattered incident beam is clearly discernable surrounding the 1.734 MeV ^{235}U NRF line.

The DINO detector system in our numerical simulations was "calibrated" using an operationally realistic procedure that involved simulating the value of the decision metric in an "open field" configuration (*i.e.* no object in the detector field of view) followed by DM simulations for a series of calibration objects with known ^{235}U aerial densities (*e.g.* 50% enriched Uranium slabs of known

thicknesses) (*cf.* Figure 5a). Since, as noted earlier, the DINO decision metric should be independent of non-resonant materials in the object under inspection, this calibration curve should be valid for arbitrary objects (*e.g.* UO₂ fuel rods, nuclear waste drums, cargo containers, *etc.*). This is confirmed in Figure 5b, where simulated DM values for a set of hypothetical Zircalloy-clad UO₂ fuel rods with ²³⁵U enrichments ranging from 0.00% ($\rho\ell_0 = 0$ gm/cm²) to $\sim 94.3\%$ ($\rho\ell_0 \sim 9$ gm/cm²) appear to follow the calibration curve quite closely.

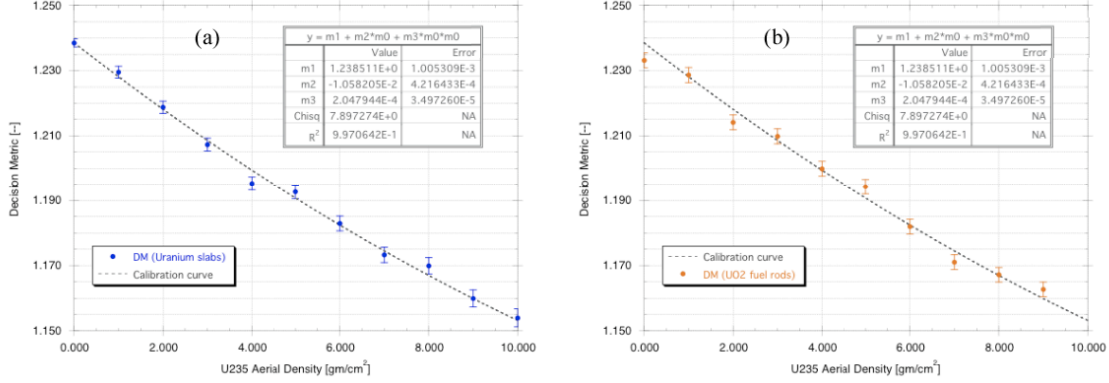


Figure 5: DINO calibration curve (*i.e.* decision metric (DM) vs. ²³⁵U aerial density). Frame (a) shows simulated calibration points along with a quadratic fit that will be used to represent the calibration curve. Frame (b) shows that simulated DM values for a set of hypothetical Zircalloy-clad UO₂ fuel rods with a wide range of ²³⁵U enrichments appear to follow the calibration curve quite closely. The error bars represent Monte Carlo uncertainties in the simulated DM values in each case (experimental DM values should show smoother trends and have much smaller uncertainties).

As an aside, we asserted at the end of the previous section that the DINO decision metric for an object which does not contain the resonant isotope (²³⁵U in this case) should be independent of both its composition *and* its effective thickness. This is confirmed in Figure 6, where Aluminum, wood and steel slabs of different thicknesses all appear to have DM values \sim DM (open field) when irradiated by our "nominal" 1.734 MeV MEGa-ray source.

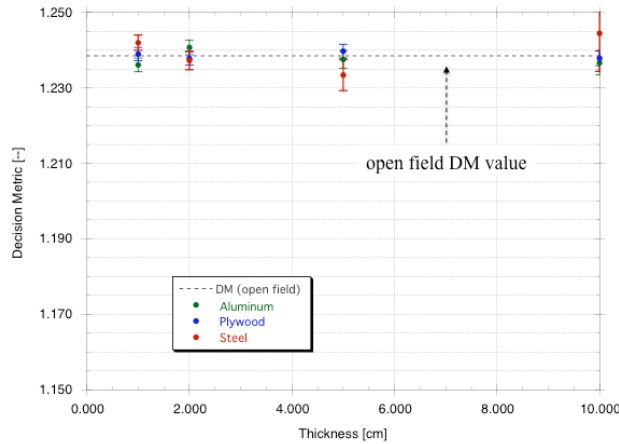


Figure 6: DINO decision metric (DM) vs. object thickness for Aluminum, plywood and steel slabs irradiated by our "nominal" 1.734 MeV MEGa-ray source. The simulated DM values for these widely disparate objects all appear to be \sim DM (open field). The error bars again represent uncertainties in the simulated DM values.

Having established a calibration curve for our DINO system, ^{235}U assay values can now be determined by inverting the measured (or, in our case, simulated) DM values for the objects under inspection (*i.e.* by deriving $\rho \ell_0$ [gm/cm²] as a function of DM). If we assume that the calibration curve can, in practice, be defined with almost arbitrary precision (*i.e.* that the statistical uncertainties in the DM calibration values can be made \ll than the uncertainties in the DM values for arbitrary test objects), then the fractional standard deviation (FSD) in the estimated value of the ^{235}U density can be expressed as

$$FSD(\rho > 0) \text{ [(dimensionless)]} = \frac{\Delta \rho}{\rho} = \frac{\Delta(\rho \ell_0)}{\rho \ell_0} = \left(\frac{1}{\rho \ell_0} \right) \left(\frac{\Delta DM}{|DM \text{ slope}|} \right), \quad (17)$$

where ΔDM is the estimated statistical uncertainty in the DM value and $|DM \text{ slope}|$ is the absolute value of the slope of the DM calibration curve. As an example, the FSD in the ^{235}U assay values for conventional UO_2 fuel rods ($\sim 3.00\%$ ^{235}U) is shown in Figure 7, where we have assumed that the incident photon flux is distributed Poisson and have estimated the evolution of the statistical uncertainties in the DM values accordingly. Under these assumptions, Figure 7a indicates that it should be possible to determine the enrichment of a fuel rod of this sort to within $\pm 3\%$ in a time span of $\sim 5 - 6$ minutes with the proposed MEGa-ray photon source (*i.e.* $\sim 10^{10}$ photons per second). Given the known limitations of passive assay techniques currently used to make such measurements, this is potentially quite impressive. Finally, it should be noted that, since $|DM \text{ slope}|$ increases rapidly as the FWHM ($\Delta E/E$) of the incident beam is decreased, MEGa-ray photon sources with narrower bandwidths should provide even better performance (*cf.* Figure 7b).

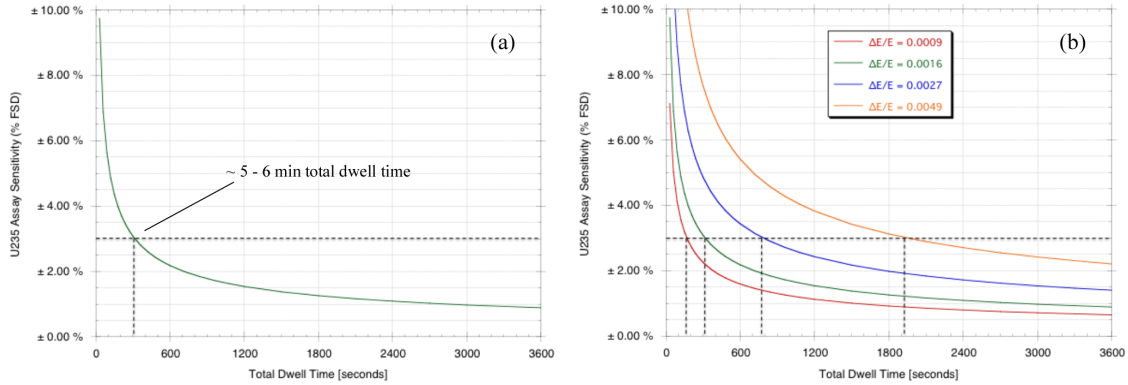


Figure 7: ^{235}U assay sensitivity (% FSD) for conventional UO_2 fuel rods ($\sim 3.00\%$ ^{235}U) vs. total dwell time (HEU foil + DU foil) with a single-stage DINO detector system. Frame (a) shows predictions for our proposed 1.734 MeV, $\Delta E/E \sim 0.0016$, MEGa-ray source operated at a nominal intensity of $\sim 10^{10}$ photons per second, while frame (b) shows predictions for MEGa-ray sources with both smaller and larger bandwidths.

Conclusions

LLNL's Nuclear Photonics Facility is expected to be capable of generating tunable, mono-energetic gamma-ray ("MEGa-ray") beams with energies of $\sim 0.5 - 2.5$ MeV and spectral intensities many orders of magnitude beyond those of current (3rd generation) synchrotron light sources. This will present serious, potentially prohibitive, challenges to the use of high-resolution (*e.g.* HPGe) detectors in NRF-based detection, imaging and assay applications; however, based on our detailed Monte

Carlo simulations, the proposed DINO NRF detection system should work quite well with planned MEGa-ray photon sources (*e.g.* $\sim 10^8$ photons per pulse at repetition rates of ~ 100 Hz with $\Delta E/E \sim 0.001$). Our simulations also predict that MEGa-ray beams and DINO detectors should be capable of providing fast, accurate assays of UO₂ fuel rods in scenarios where other assay techniques might not be as reliable or even feasible (*e.g.* highly-radioactive spent fuel assemblies).

We note that the discussion here has been limited to single-stage DINO detector designs. We have also investigated two-stage DINO designs in which independent, sequentially-aligned scintillators are used to record the responses of first the resonant, and then the non-resonant witness foil. Two-stage designs have both advantages and disadvantages when compared to single-stage designs, all of which will be discussed in a forthcoming publication.

Acknowledgements

This work was performed under the auspices of the U. S. Department of Energy by Lawrence Livermore National Laboratory (LLNL) under Contract DE-AC52-07NA27344.

References

- [1] C. P. J. Barty, M. B. Aufderheide, K. S. Budil, G. J. Caporaso, J. M. Hall, F. V. Hartemann, E. P. Hartouni, W. E. King, D. P. McNabb, B. Rusnak, C. W. Siders, J. E. Trebes, "Precision Mono-Energetic Gamma-ray (MEGa-ray) Science for NNSA Missions", LDRD 09-SI-004 (LLNL, 2009); C.P.J. Barty, private communication.
- [2] W. Bertozzi, S. E. Korbly, R. J. Ledoux and W. Park, "Nuclear resonance fluorescence and effective Z determination applied to detection and imaging of special nuclear material, explosives, toxic substances and contraband", *Nuc. Inst. & Meth.* **B261**, 331 (2007).
- [3] M. S. Johnson, C. A. Hagmann, J. M. Hall, D. P. McNabb, J. H. Kelley, C. Huibregtse, E. Kwan, G. Rusev and A. P. Tonchev, "Searching for Illicit Materials using Nuclear Resonance Fluorescence Stimulated by Narrow-band Photon Sources", LLNL-JRNL-422898 (LLNL, 2010); under review for publication in *Nuc. Inst. & Meth. B* (2011).
- [4] F. R. Metzger, "Resonance Fluorescence in Nuclei", *Prog. in Nuc. Phys.* **J1**, 54 (1959).
- [5] W. Bertozzi, *et al.*, U.S. Patent # 2006/0188060 A1 (2006).
- [6] R. Buck, E. Lent, T. Wilcox and S. Hadjimarkos, *COG: A Multi-particle Monte Carlo Transport Code*, UCRL-TM-202590 (LLNL, 2002), *cf.* <http://cog.llnl.gov/>; available through the Radiation Safety Information Computational Center (RSICC) at Oak Ridge National Laboratory (<http://www-rsicc.ornl.gov/>) as code package C00777 MNYCP 00 (*COG 11: A Multi-particle Monte Carlo Code System for Shielding and Criticality Use*).
- [7] F. V. Hartemann, F. Albert, S. G. Anderson, D. J. Gibson, R. A. Marsh, S. Q. Wu, C. P. J. Barty, "Optimization of Compton Scattering for NRF-based Nuclear Materials Management with MEGa-rays", published in *Proc. INMM, 52nd Annual Meeting* (Palm Desert, CA, 2011).